ELSEVIER

Journal of Chromatography A, 675 (1994) 155–175

JOURNAL OF CHROMATOGRAPHY A

Multichannel chromatography and on-line spectra from a flame photometric detector

Brian Millier, Xun-Yun Sun[1], Walter A. Aue*

Department of Chemistry, Dalhousie University, Halifax, Nova Scotia B3H 4J3, Canada

(First received November 9th, 1993; revised manuscript received March 23rd, 1994)

Abstract

A rotating variable interference filter has been incorporated into a flame photometric detector to acquire and simultaneously display low-resolution spectra that are diagnostic for eluting peaks. In its present form this approach yields ten chromatograms (for ten different wavelength segments) that are stored in the computer for subsequent data manipulation such as baseline correction and curve smoothing; three-dimensional display; peak and noise diagnostics; and magnification, subtraction, or elemental correlation of chromatograms. A third, spectral dimension is thus added to the conventional two, chromatographic dimensions of retention time and analyte intensity. The three-dimensional performance is at present accompanied by an order-of-magnitude loss in detection limit and linear range. Typical one-segment (*i.e.* 5% dwell time) elemental detectabilities, at $S/N_{p\text{-}p} = 2$, are $7 \cdot 10^{-13}$ g P/s (via HPO*), $3 \cdot 10^{-11}$ g S/s (S_2^*), $7 \cdot 10^{-12}$ g Ge/s (GeH*) and $4 \cdot 10^{-12}$ g Ru/s.

1. Introduction

As texts on instrumental analysis are fond of pointing out, chromatography and spectroscopy are complements, not competitors, by nature. Chromatography separates but rarely identifies compounds; spectroscopy performs the opposite role. Significant analytical advances can therefore result if the two techniques are properly joined.

But analytical advances can result not only from two instruments symbiotically joined, they can also result from one instrument parasitically enriched (as in this study). It is not surprising, then, that practitioners of either chromatography or spectroscopy should have sought to lend their favourite technique certain features that, in effect, imported or imitated the strength of the other. This may have involved the improvement of dispersion and/or the addition of a further physical or chemical dimension. Instruments offering several dimensions (sectors, channels, columns, etc.) have indeed become commonplace.

Nor is the advantage of multidimensional operation restricted to chromatography and spectroscopy. Other types of reactive and unreactive flow systems on one hand, and sensing systems based on mass, radiation, electron exchange, etc., on the other, have similarly benefitted. As a consequence, the fundamental and technical resources on which this study is able to draw are far too general and numerous to list in any detail. Suffice it to state that both concept

* Corresponding author.

[1] Present address: Environmental Trace Substances Centre, Room 207, University of Missouri–Columbia, Sinclair Road, Columbia, MO, USA.

0021-9673/94/$07.00
SSDI 0021-9673(94)00294-J

and execution of this specific project rely on ample and, we hope, obvious precedents.

Our specific project was to obtain spectra from analytes as they pass through the flame photometric detector (FPD) [1–4]. This well-known detector monitors luminescence, but it does not measure its spectral distribution during analysis. Yet, with some twenty elements now known to respond in the FPD —and further ones likely to follow suit— instantaneous acquisition of spectra from eluting peaks could be of significant value: for the injection of one-shot-only samples, for compound confirmation or identification, for selective multi-element determination, and so forth. The potential merit of adding spectral information to the response of the FPD increased vastly when this detector expanded its purview from volatiles to non-volatiles, *i.e.* from gas chromatography to liquid chromatography, supercritical fluid chromatography and capillary electrophoresis (as well as to various non-chromatographic monitoring techniques).

We did not want to join a typical *spectrometer* to the gas chromatograph; this has been done before in various ways and with varying degrees of success. Rather, we wanted to take the simplistic approach of modifying the FPD so that it could procure spectra on the side and on the fly.

Procuring spectra on the fly is, however, quite difficult. The difficulty lies in the very low intensity and the short duration of the luminescent episodes that constitute the peaks of a chromatogram. The FPD differs strongly in this regard from systems that radiate more intensely (where, for instance, multisensor arrays may be used); or from systems that can be arrested in time (where, for instance, an analyte peak trapped in the detector cuvette may be repeatedly scanned to determine its absorption or fluorescence spectrum).

Under analytically relevant conditions, then, weak spectra in the FPD are difficult to obtain even from continuous analyte inputs. Gleaning them from peaks that stay in the detector for only a few seconds raises that level of difficulty by orders of magnitude.

Furthermore, if spectral information is to facilitate such analytical tasks as the assessment of peak purity, the correction of background radiation, and the correlation of wavelength-dependent chromatograms, the spectra have to be acquired at a rate that is much faster than the peak's passage through the detector. Roughly but typically, 10-s chromatographic peaks thus require 1/10-s spectral scans. It would appear that the simplest, least expensive, and (in terms of light throughput) most efficient means of procuring spectral information should be a rotating variable interference filter.

If such a filter is used to monitor response at different wavelength ranges every tenth of a second, the filter wheel must revolve at 600 rpm. How many samples should reasonably be taken during one of its revolutions —*i.e.* how broad should be the discretely monitored wavelength regions— depends on the bandpass of the filter, the width of the beam, and the ability of the monitoring system to accommodate the data influx. Not only does the monitoring system —a photomultiplier tube (PMT) with high-speed amplifier and dedicated computer— have to record the data, but it also has to prepare them for simultaneous appearance on the screen.

The screen should display the immediate spectrum together with the developing chromatogram, and both need to be smoothed for convenient viewing. Beyond the acquisition phase discussed in this report, the algorithms must also be capable of handling a wide variety of chromatographic and spectral manipulations of the stored raw data, such as integration, subtraction, correlation, normalization, baseline correction, digital smoothing, three-dimensional display, spectral comparison, noise analysis, etc.

Given these demands, it seems reasonable to limit each file at the outset to about half an hour of chromatographic acquisition time, and to restrict the number of spectral segments to ten (a combination that already comprises about $2 \cdot 10^5$ raw data points). The optical bandpass of the variable filter wheel (17 nm maximum between 400 and 700 nm) would easily support a higher number of spectral segments, but ten channels are considered adequate for a first try. If successful, that try should allow a more knowledgeable,

hence more refined choice of time and wavelength parameters in subsequent designs. Besides, the measure of success at this stage is not how close the new spectral information comes to the performance of a conventional spectrometer, but how much it adds to the capabilities of the FPD. Spectra, *per se*, are not the objective; the analytical information that can be obtained from them, is.

This project, coming as it does from an academic realm of characteristically limited means, became feasible only through recent developments in the hardware and software capabilities of personal computers (PCs). In this context we intend, by choice as well as by necessity, to keep the price tag of additional components significantly below the price of a simple, single-channel FPD.

Equally commensurate with academic means is the decision to design and build the acquisition system in a series of *modular* components, so that these could be used individually for other layouts, assemblies and purposes. As one illustrative example of this strategy, the rotating filter wheel and the high-speed signal acquisition assembly could be used to transmit data not only to a computer but also to a digital storage oscilloscope. This oscilloscope could sum and read the data —from passing peaks if need be but more importantly and typically from a *continuous* input such as a stream of analyte, a background emission, a non-chromatographic sensor signal or, for that matter, any long-term luminescence phenomenon— with (close to) the best resolution of which the variable interference filter is capable.

Given the low *absolute* light intensity of the chemiluminescence, the inherent optical limitations of the interference filter, the longer distance and hence the narrower direct-light transmission cone from the flame to the PMT (a cone that is, furthermore, severely restricted by the mandatory filter aperture), it seems that some use of inexpensive optical devices is required to boost the light throughput and bring it closer to that of a conventional FPD channel.

Mirrors [1,5] and lenses [5,6] have been used in some FPDs, although most modern models favour direct observation of the flame (and that for good reason). The inclusion of optical elements is of little help, sensitivity-wise (*cf.* ref. 7), if the noise is mainly due to flame flicker or chromatographic fluctuations.

In our case it is not. However, the merit or demerit of adding a mirror and/or a lens is still not as easy to predict as it would be for a more conventional type of spectroscopy. One of the reasons for that is the shape of the FPD flame or, more to the point, the space the various luminescences occupy. That space depends not only on the obvious conditions of flow-rates and burner dimensions, but also on the nature of the analyte element, on the various emitters from that element (if there are more than one), and, quite disturbingly, on the amount of analyte —not to mention the nature and amount of various co-elutants and contaminants.

The luminescences associated with chromatographic peaks are unique and fascinating spectacles to watch: the variation of their colours and shapes seems infinite. The luminescent space can vary from lanceolate to ovoid, to prolate and oblate spheroid, and even to spherical and cylindrical (the latter, for instance, in the case of a surface luminescence on the quartz chimney); it can also fill *all* of the accessible FPD interior. The volume of the luminescent space can thus change from a few to a few thousand mm^3 (under the same flow conditions!). For instance, the blue luminescence of sulphur can sometimes be observed to appear —vague, weak, and seemingly out of nowhere— in the whole detector volume (peak start); then become stronger and contract into a brilliantly blue flame at the detector jet tip (peak apex); then again weaken in intensity, diffuse all over the detector volume, and slowly fade out (peak end). The theoretical explanation for this phenomenon is straightforward, given the second-order kinetics of the blue S_2 bands, but its enhanced detection via mirrors or lenses is not. The second-order kinetics of sulphur may be regarded a special effect, but first-order emitters, too, can be surprisingly varied in the size and shape, layers and colours of their luminescences. This distinguishes the FPD from the usually much larger, high-energy

flames and plasmas of atomic emission spectroscopy, whose visible shape is changed but little by the presence of analyte.

Thus, the old spectroscopic motto: "project the image of the flame onto the aperture" may be difficult to follow in the case of the FPD. The best one can hope for is to collect a reasonably large portion of light from the polymorphous luminescences and pass most of that light, in as concentrated a beam as possible, through the filter and on to the PMT. The desideratum here is not projection but power, not image but intensity.

2. Experimental

The circular variable interference filter was (initially) positioned between the cooling coils and the PMT of the same Shimadzu FPD we had been using for the last two decades (a Shimadzu GC-4BMPF). The circular filter rotates in a light-tight casing with 1-in. (1 in. = 2.54 cm) diameter entrance and exit ports. The PMT output is processed by (1) a separate high-speed, high-gain amplifier assembly, and then forwarded to (2) the data acquisition circuitry located inside (3) the computer. These three discrete units, as well as some simple optical devices for adjusting the light beam, will be described anon.

First, however, we need to mention the rationale behind the division of circuitry elements into three discrete units. To minimize noise, the high-speed PMT amplifier is given its own shielded enclosure and dedicated power supply. The only other circuit in the amplifier assembly is a minor one, providing power to the optical switch. This unit, which is located in the filter wheel assembly, provides a synchronization signal. The filter wheel assembly includes an integral speed control circuit to stabilize the rotational speed of the wheel. When set up in this fashion, these two units could be interfaced to, for instance, the earlier mentioned digital storage oscilloscope for better spectral resolution. Here, though, they are connected to a custom-built data-acquisition board that, by virtue of residing directly on the PC's ISA bus, allows fast data collection.

2.1. Filter wheel assembly

The filter wheel (item 57496; Oriel Corporation, 250 Long Beach Boulevard, Stratford, CT 06497, USA) is a 4-in. diameter disk with a semicircular variable interference filter section that, over 172° at a dispersion of 1.75 nm/degree, covers the 400–700 nm wavelength range with a 17-nm maximum bandpass and a 15% minimum transmission (according to Oriel specifications). The 180° opaque section acts to balance the wheel for spinning. A filter unit encompassing the full 360° would have been more desirable in terms of higher resolution and proportionately longer light collection, but such a filter is not available "off-the-shelf" to the best of our knowledge.

The filter housing uses two matching square pieces of aluminum stock, machined out to accommodate the filter wheel inside. The wheel rotates past the 1-in. diameter input and output (PMT) ports, both of which are partially covered by two, roughly vertical strips of black tape that run parallel to the filter radius (*i.e.* along isochromes) and form the desired aperture between them. The wheel is mounted on a 1/4-in. shaft held by a double-bearing assembly, and is turned by a small d.c. motor (with integral tachometer) via two pulleys and a flat belt. The ratio of the motor pulley to the filter pulley is 0.263, *i.e.* a motor speed of 2281 rpm produces the desired filter speed of 10 revolutions/s.

The rotational filter speed is very stable, owing to the motor and speed control board taken from an old Tandon 5-1/4 floppy disk drive assembly. (This type of assembly was used in the extremely popular IBM PC and is now available for next to nothing through many outlets.) The stability of rotation is based on the combination of the tachometer (built into the motor) and the pulse-width-modulated feedback controller. The 12 V d.c. needed to drive the motor/controller are provided by a dedicated 12 V, 1.5 A power supply.

A small optical switch assembly is positioned

opposite, *i.e.* 180° from, the light beam. When the filter wheel rotates to a position that allows light to pass from the inlet port to the PMT port, the optical switch finds its light path blocked, resulting in the change of signal state needed to trigger data acquisition. The trigger pulse occurs at the transparent-to-opaque transition, *i.e.* when, on the opposite side, the 400 nm edge of the variable filter just passes the centre of the inlet/PMT ports. This means —given equal time slices for observing each wavelength region— that the first segment will collect only about half the light that would be needed for a quantitative comparison of its intensity with that of subsequent segments. This boundary distortion (which owes its existence to an initial design flaw) could be corrected in either software or hardware, particularly if the spectral profiles of various emitters need to be retained in the form familiar to most analysts.

2.2. High-speed, high-gain PMT pre-amplifier assembly

Fig. 1 describes the pre-amplifier assembly. An OP-07 operational amplifier is used for current-to-voltage amplification. The gain at this stage is 10^8 V/A. Bucking current is introduced through a 1000-MΩ resistor to the input of this amplifier. A 10-turn potentiometer adjusts the bucking current to accommodate various possible PMTs and the range of voltages used to drive them.

A second stage of amplification provides a further gain of 10 as well as a polarity inversion: the latter results in the negative output signal the data acquisition assembly expects.

A built-in power supply serves both the pre-amplifier and the optical switch in the filter wheel assembly. Also, a single resistor is used as a load for the phototransistor in the optical switch. As mentioned earlier, the circuit is designed to allow the filter wheel and the pre-amplifier to operate independently of the data acquisition assembly. This permits the instrumentation to be used for other purposes, *e.g.* for feeding purely spectral data of higher resolution to a suitable collection and readout system.

2.3. Data acquisition assembly

This functional block is custom-designed owing to the somewhat unusual requirements of the rotating filter wheel. Some of these requirements are:

(1) The unit has to be able to synchronize its data collection with a single trigger pulse per revolution of the wheel.

(2) The digitization of the PMT signal has to comprise (in time) essentially all of the particular filter segment that is being monitored by the PMT tube. This appears necessary because the light capable of reaching the PMT through the 1-in. diameter beam containment, the focussing lens, the aperture(s), and the variable interference filter is already very low; and it is further reduced by a factor of 20 for each segment (in the case of a 10-segment acquisition from a filter wheel that is 50% opaque). A gated integrator is used in that function, followed by a fast 12-bit analog-to-digital converter.

(3) The unit has to accommodate a wide dynamic range of signals; hence offers a computer-controlled gain circuit.

Fig. 2 shows the data acquisition assembly, which is based on a JDR Microdevices PR-2 prototype board. This is an 8-bit PC board with all buffering and decoding circuitry already present, including the well-designed power and ground planes necessary for proper analog operation. The 8-bit board was chosen because most of the peripheral integrated circuits (ICs) are 8-bit devices.

The timing circuitry will be discussed first. Its heart is an 8253-5 programmable interval timer, U9. This IC contains three 16-bit counter/timers, all of which are clocked by a 1.0-MHz quartz module, U1. Timer 1 is turned on by the synchronisation signal from the filter wheel (after conditioning by Q1 and U5:A, an inverter). The output of timer 1 consists of ten 1.0-μs pulses, one for each segment. The actual number of pulses can be changed in software: *ten* segments happens to be the initial, arbitrary choice of this study. The ten pulses then (a) set the flip-flop U8:A and generate an interrupt to the PC, and (b) trigger (through gate U5:D and inverter

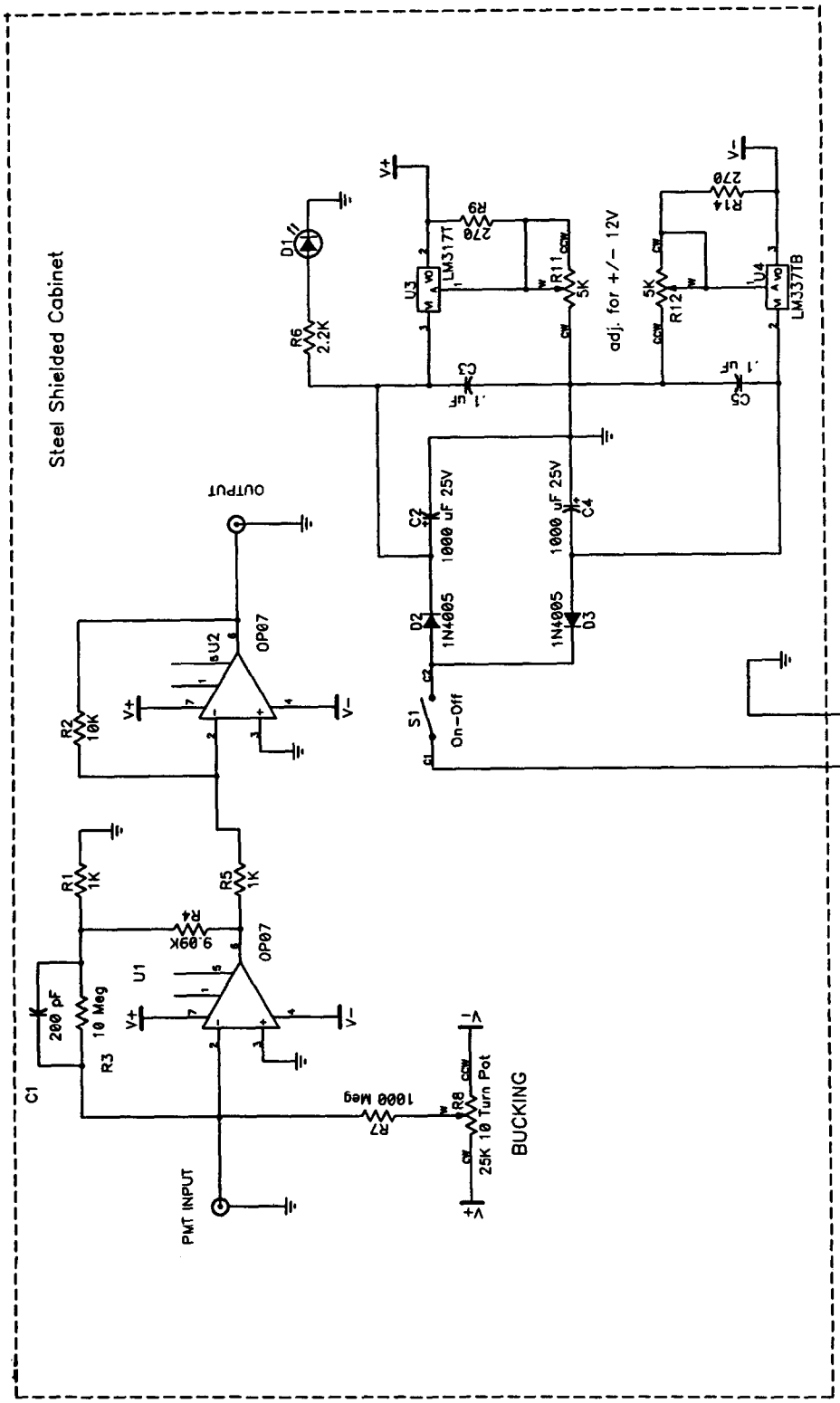

Fig. 1. Amplifier assembly. K = kΩ; Meg = MΩ; AC = alternating current; 10 Turn Pot = ten-turn potentiometer.

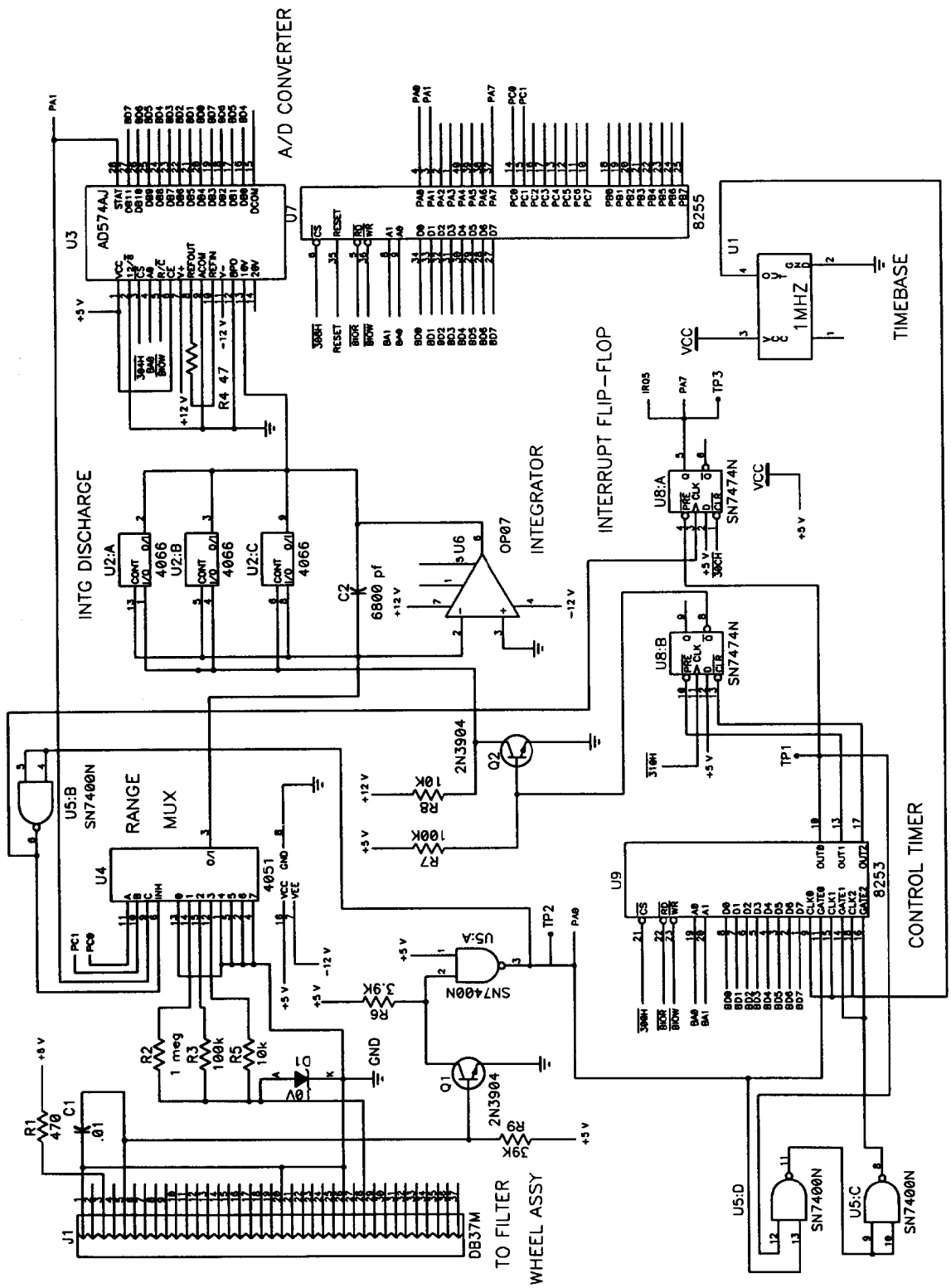

Fig. 2. Data acquisition assembly. k = K = kΩ; pf = pF; meg = MΩ; resistors without units indicated are in Ω; GND = ground. Note: circuit built on a JDR 8-bit prototype card Model JDR-PR2.

U5:C) timers 2 and 3, which are configured as programmable monostables. Each of the timers uses a different delay time, the net result being that the flip-flop U8:B will discharge the integrating capacitor for a fixed time after U3, the analog-to-digital converter (ADC), has completed its job. The actual command to perform the conversion is provided by a "write" to the ADC, initiated by code in the interrupt service routine, and triggered when U8:A asserts the IRQ5 line to the PC.

The signal path will be discussed next. The low-level current from the PMT is amplified externally by the high-speed pre-amplifier assembly and enters the data acquisition board as a signal of negative polarity. A zener diode, D1, limits this signal to a range of +0.6 to −10 V. An analog multiplexer IC, U4, is used in conjunction with three resistors, R2, R3 and R5, to select three sensitivity ranges with decade spacing. With the chosen integration time of 5 ms (less capacitor discharge time) and an integration capacitor of 6800 pF, the 10-V full-scale ADC input is reached with input voltages of 13.6, 1.36 and 0.136 V. The actual integrator comprises the OP-07 operational amplifier, U6, and the 6800 pF capacitor. A quad bilateral CMOS switch, U2, is used to discharge the capacitor. Since U2 operates from a +12 V supply, Q2 is needed as a level shifter to provide enough voltage for control of U2.

The output of the integrator feeds directly the +10 V input of the AD574AJ ADC. The busy-status output of the ADC is monitored via input port A of U7, an 8255 parallel peripheral interface (PPI) IC. While the ADC is performing the conversion, the status output is high: this signal is fed to an address input of U4, the input multiplexer, which in turn feeds a zero volt signal to the integrator to keep it constant during A/D conversion. As well, U5:B feeds the inhibit input of the multiplexer with the result that the integrator is disconnected from any signal while the opaque half of the filter wheel intercepts the light beam.

Two bits of output port C (U7), namely PC0 and PC1, are used to set the multiplexer address, thereby setting the integrator gain in three decade-related steps.

2.4. Software

The software operates in two discrete sections for (1) the acquisition stage and (2) the manipulation and documentation stage. This division of labour is not arbitrary but owes its existence —primarily though not exclusively— to the different technical demands placed upon hardware and software by two disparate operational stages.

Above all: during the acquisition stage the computer must collect the data coming from the filter wheel quickly and reliably. This task requires an interrupt service routine. The routine must have a very short latency time (the maximum time the data acquisition hardware has to wait before the host computer "services" it). It must also have a high priority so that it is never disabled or "masked out" for any length of time. For this reason we use a compiled QuickBasic program in conjunction with an assembly language interrupt service routine driver, running under DOS-5 or -6. (Our attempts to write software running under Microsoft Windows 3.1 were unsuccessful: Windows is a non-preemptive multitasking system —resulting, occasionally, in an interrupt latency time too long for this application, and thereby causing the loss of data and synchronization with the filter wheel.)

No such time constraints exist in the manipulation/documentation section of the software. The many advantages of the Microsoft Windows environment clearly favour it for this application. We chose to use the Visual Basic language, running under Windows. Some of its advantages are: (1) access to a multi-window graphic user interface (GUI), (2) support for different printers/plotters providing hardcopy output and (3) support for numerous large arrays that are limited only by (in our case) 8 megabytes of installed memory.

Data are transferred from the acquisition program to the manipulation/documentation program using files. Owing to QuickBasic's binary file size limitations, a single run (ten parallel chromatograms) is saved as ten separate segment files all sharing the same primary filename. This name is also used for an appended file containing the operator's "yellow notepad" (which actually

appears on the screen in bright yellow colour, demanding that experimental conditions be properly recorded).

2.5. Computer

The acquisition and manipulation software makes use of the following hardware: (1) an Intel 486-class central processing unit (CPU) running at 33 MHz with 8 megabytes of memory, (2) a video local bus (VLB) VGA Video card to speed up the graphics display (about four times), (3) a 120 megabyte (15 ms access time) hard disk drive that, with the DOS-6 disk-doubling software, provides about 230 megabytes of disk space for the large files, and (4) a "15-in." NEC VGA monitor that displays the graphics in colour and with adequate resolution. (Item 1 is required for acquisition, while items 2 through 4 are used primarily for ease of operation.)

2.6. Data smoothing

Data smoothing is available either from an unweighted moving-average called "AVG" (an extremely simple but still highly effective filter that requests the operator's definition of the number of surrounding signals to be considered for each data point, and that is offered both for the acquisition screen and the full manipulation stage); or through a Hamming-window type "FIR" (finite impulse response) low-pass digital filter with fully variable cut-off (that, because of its longer processing time and —for our particular chromatograms— only marginally better performance, is supplied at the manipulation stage only). The FIR digital filter gives the operator the choice of a cut-off frequency and the choice of 32, 64 or 128 taps for different filter "orders". Of the three, the 128-tap filter provides the sharpest cut-off, of course, but it also requires the longest processing time: about 40 s for one typical segment, *i.e.* for one fixed-wavelength chromatogram of *ca.* 20 min duration. In the manipulation mode, the moving-average-filtered chromatogram can be saved for later treatment. In the acquisition mode, however, it is abandoned as the screen image fades and only the *raw* data are stored in the computer's memory (a process that differs from the behaviour of some chromatographic integrating systems or, for that matter, from the behaviour of the human brain).

For sensitivity comparisons, data are smoothed by two conventional treatments: the FIR digital filter as described above, or an analog ("RC") filter. The latter, used here between Shimadzu electrometer and recorder, is a conventional, simple three-pole filter, that offers a series of time constants in the 0.1–10-s range (Fig. 3). Both filters are set such that only a small (less than 10%) reduction in peak height occurs.

2.7. Optical layout

As discussed in the Introduction, maximizing light throughput and minimizing the spread of the beam at the plane of the variable filter is an act of necessity. It is also a matter of compromise for different detector conditions and analytes, at least if inexpensive optical elements are to be used in essentially fixed positions. Fig. 4 shows a schematic of the simple layout that is being used in this study.

To facilitate the use of inexpensive optical components, the FPD flame is raised to the centre of the *ca.* 1-in. diameter cylindrical light path. To improve light transfer through the tunnels, ports and apertures, a first-surface mirror ($f = 10$ mm, 25 mm diameter, item 43 464; Edmund Scientific, 101 E. Gloucester Pike, Barrington, NJ 08007-1380, USA) is held, and moved to the most advantageous position behind the flame, by a laterally adjustable piston. To narrow the effective optical bandpass, a double convex lens ($f = 25$ mm, 25 mm diameter, Edmund Scientific 32 490) is installed at about focal distance from the front side of the rotating filter. The head-on PMT is mounted close to the filter's back side in order to intercept most of the light beam. (Fig. 4 suggests that the PMT should be mounted closer still: this mount awaits the next progression of the wheel.)

Fig. 4, while to scale, is nevertheless approximate. The light rays (which are drawn here for viewer's convenience only) appear to originate from a point source rather than from a vaguely defined and often shapeshifting luminescence.

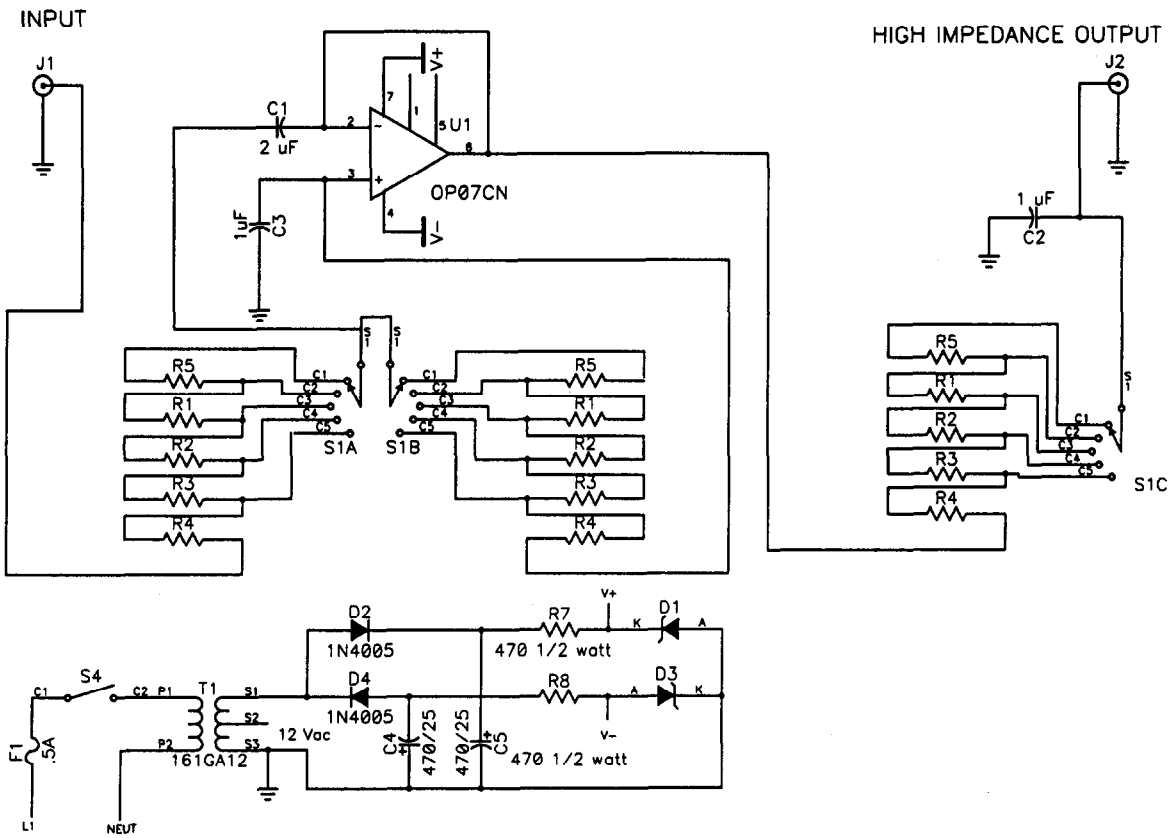

Fig. 3. Analog filter. R1 = 1.5 MΩ; R2 = 680 kΩ; R3 = 680 kΩ; R4 = 8.2 kΩ; R5 = 2.2 MΩ; C1 = 2 μF; C2 and C3 = 1 μF.

To make up for these vagaries, the back mirror can be moved back and forth —from the outside and under operating conditions— in order to optimize light throughput on an empirical basis for different elements and conditions.

2.8. Miscellaneous

The FPD's Hamamatsu R-374 PMT is driven by (typically) −700 to −900 V from a laboratory-built −70 to −1270 V power supply. Separations are carried out on a several-years-old 100 × 0.3 cm I.D. borosilicate column packed with 5% OV-101 on Chromosorb W, 100–120 mesh (150–125 μm) and operated with *ca.* 26 ml/min of nitrogen carrier gas. Injections of tetraethyllead are used as needed to reduce the background luminescence, particularly when the quartz chimney is installed.

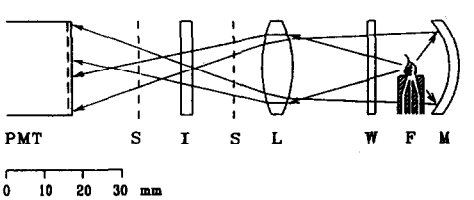

Fig. 4. Optical layout. PMT = photomultiplier tube; S = slit; I = interference filter; L = lens; W = window; F = flame; M = mirror.

In this study the detection limit is determined for a *single* segment. However, it can just as easily be determined for the "total" chromatogram (*i.e.* the sum of ten segments); or for any combination, subtraction or correlation chromatogram. The computer offers "DL" ("detection limit") routines for both amount and flow; these are based on either the root-mean-square calculation or the peak-to-peak measurement of the baseline noise, at the two common signal-to-noise (S/N) ratios of 3 and 2, respectively.

Thus, for the more lenient $S/RMS = 3$ definition,

$$DL = 3 \cdot \frac{RMS}{S} \cdot A \text{ (g or mol)}$$

or

$$DL = 3 \cdot \frac{RMS}{S} \cdot \frac{A}{w_{60.7}} \text{ (g/s or mol/s);}$$

and for the much stricter $S/N_{p\text{-}p} = 2$ definition,

$$DL = 2 \cdot \frac{N_{p\text{-}p}}{S} \cdot A \text{ (g or mol)}$$

or

$$DL = 2 \cdot \frac{N_{p\text{-}p}}{S} \cdot \frac{A}{w_{60.7}} \text{ (g/s or mol/s);}$$

where S is the signal (peak height), RMS is the root-mean-square noise of the baseline (equal for Gaussian noise to σ_b), A is the amount injected (in g or mol), $w_{60.7}$ is the width of the peak (in s) at 60.7% of its height (equal in a Gaussian peak to $2\sigma_p$) and $N_{p\text{-}p}$ is the peak-to-peak fluctuation of the baseline, with drift and spikes excluded.

3. Results and discussion

3.1. Data acquisition vs. data manipulation

This report deals with the primary process —data acquisition and simultaneous presentation— of what may be termed "time-multiplexed non-dispersive spectrometry" [8] of chromatographic effluents. As discussed, the secondary process (data manipulation) is both conceptually and physically separate, and will be touched in this report only as far as is necessary to characterize the performance of the "three-dimensional" (3-D) FPD and its data acquisition system.

There are several reasons why data acquisition and data manipulation are treated as two different processes. The main reason, at least for this study, is electronic and has been mentioned in the Experimental section: During a sample run —*i.e.* while the present computer is acquiring chromatographic-cum-spectral ("chromspec") data and, after smoothing, is displaying them as moving averages on the screen— it is fully occupied with that task.

But there are also reasons of a non-electronic nature for distinguishing between the acquisition process and the manipulation process (two processes as different in time and effort as catching a rabbit and cooking it). For instance, the physical separation of the two stages offers the operator the chance to attain the desired balance between time spent watching the chromatogram taking shape and being recorded on one computer, and the time spent scanning and perhaps manipulating separations that have been stored earlier on another computer. As it happens, different laboratories differ greatly in the fraction of time they allocate to these two distinct types of activity. Such time allocation depends on whether the particular brand of chromatography involves routine analysis, analytical development, or exploratory research; whether it runs automatically, requires occasional attention, or calls for human intervention in the separation process; and even whether it takes place in a civil-service, industrial or academic setting.

Yet another reason for separating the acquisition from the manipulation-cum-documentation functions is conceptual and concerns the potentially much wider use of the still developing methodologies. A rotating circular variable interference filter pretty well needs its own specialized acquisition algorithm. However, such a filter could also be used in various other types of luminescence monitoring. Furthermore, such a filter is only one of the many potential multichannel signal sources, including some non-optical and non-chromatographic ones, that could benefit from the diagnostic, preparative and descriptive capabilities of the growing manipulation software[a] (into which Windows-based adaptations of our earlier algorithmic efforts [9–11] might eventually be incorporated).

[a] Researchers interested in these programs for non-commercial purposes are invited to contact the first author for source codes and/or copies.

3.2. Operator controls

While the data acquisition functions are (and, given the fleeting nature of their task, must be) automatic, most of the data manipulation functions are interactive. The experienced operator, [whose recognition of chromatographic and spectral shapes (signal and noise patterns) is superior to that of the computer, and whose common sense and analytical motivation are essential for the task] is allowed wide latitude in measuring, correlating, manipulating, interpreting and reporting of data. The transitory acquisition functions must therefore safely commit to memory *the complete set of raw data* —although the simultaneous appearance of both the chosen-segment chromatogram and the prevailing spectrum uses simple moving averages to quiet an otherwise agitated screen. The operator is given the choice of the number of data points to be averaged (how wide to open the window) and will do so with the expected peak width and baseline noise in mind; the operator is also given the choice of the particular segment (which wavelength region to look at) and will do so in accordance with the nature of the sample and the purpose of the analysis.

It is also possible for the operator to specify, in either acquisition or manipulation mode, a weighting factor for each spectral segment. This routine can produce spectra that are roughly corrected for the response profile of the PMT and the transmission characteristics of the variable filter, as well as for possible border effects (*i.e.* effects relating to total light throughput, wavelength gradation and spectral cut-off) in the first and/or last spectral segment. Its formal attractiveness notwithstanding, the primary merit of this intensity-weighting routine is spectroscopic rather than chromatographic.

3.3. An alternative approach to data acquisition

Despite the success of the electronic approach taken in this study, we believe that the many advantages of the Visual Basic/Windows environment should not remain restricted to the (slow) manipulation program, but should be made available to the (fast) acquisition program as well. We assume that this could best be accomplished by using a microprocessor-based data acquisition controller, either in the form of a free-standing unit interfaced to the host computer via a serial RS-232 or IEEE-488 data link, or in the form of a board built into the host computer (as in the present unit). This would eliminate the critical timing constraints that have so far made it impossible to run Visual Basic under Windows for data acquisition. If the QuickBasic limitation were removed, the data acquisition arrays could become much larger and allow higher optical resolution through the use of a larger number of spectral segments.

3.4. Visual system performance

How well does the on-line system perform? It is difficult to depict for documentation purposes the visual display offered by the data acquisition program, because photographs of the CRT screen are of notoriously poor quality. As a substitute, a "window dump" of the manipulation mode's "SCOUT" routine is exhibited here in Fig. 5. The acquisition mode's developing chromatogram and its spectral vignette look very much the same —except for being coloured on the screen and, of course, for terminating there at the arrow marking the present.

The SCOUT routine of the manipulation program allows the operator to move said arrow (in cursor form) along a stored chromatogram and watch the spectra of peaks pop up accordingly: this routine can serve as an operator-controlled recapitulation of what had happened initially and automatically in the ephemeral acquisition process. It is easy for the experienced operator to watch the "spectra" change in real time and recognize the FPD-active elements of peaks passing through the detector in the acquisition mode; or to follow SCOUT's arrow in the similar pursuit of peaks passing through the algorithmic gate in the manipulation mode. In Fig. 5, the peak marked by the time arrow (cursor) is that of tetramethyltin and the spectral window accordingly shows the green SnOH and the red SnH emission —albeit only in the form of ten

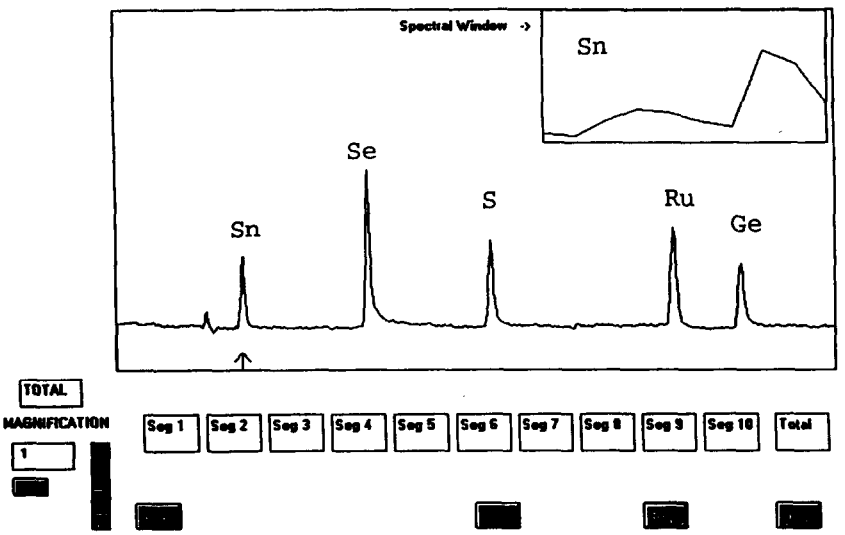

Fig. 5. Chromatogram and spectrum, similar to screen image seen during data acquisition. First segment intensity multiplied by two (see text for further explanations). Compounds: Sn = tetramethyltin; Se = dimethyldiselenide; S = di-*tert.*-butyldisulphide; Ru = ruthenocene (dicyclopentadienylruthenium); Ge = tetra-*n*-butylgermane. Hydrogen 50 ml/min, air 40 ml/min.

segment intensity points connected by *straight* lines (with the first datum, from *ca.* 400 nm, and the last datum, from *ca.* 700 nm, located in the window frame).

Fig. 6 records further the spectral windows as SCOUT's arrow targets the next four peaks of Fig. 5. These peaks are due to dimethyldiselenide, di-*tert.*-butyldisulphide, dicyclopentadienylruthenium and tetra-*n*-butylgermanium. Their "spectra" are hence characteristic of selenium (Se_2), sulphur (S_2 plus a trace of HSO at the red border), ruthenium (emitter unidentified but possibly RuH) and germanium (GeH).

(Note that it may be preferable —and less objectionable to spectroscopists proper— to speak here of "spectral envelopes" rather than of "spectra". A rough summation of the combined effects of filter bandpass, port apertures and segment scan time shows the effective half-height bandpass to be typically in the 60-nm range. Since the formal segment is only 30 nm (18°, 5 ms) wide, this means that the wavelength regions of the ten actually monitored segments do overlap considerably: a consequence of collecting light as much and as long as reasonably possible. Yet this matters little in terms of elemental recognition: the resulting spectra, though broadened by acquisition and cornered by display, are nevertheless well reproducible and therefore diagnostic of their parent ele-

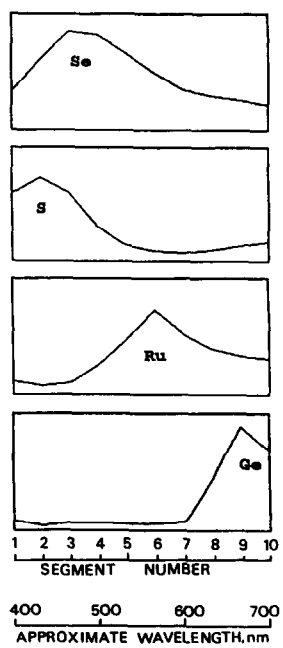

Fig. 6. Spectral windows as obtained by moving the SCOUT arrow (cursor) through four peaks of Fig. 5.

ments. The wheel turns for elemental recognition, not spectral definition: *other* methodologies should be chosen if a heretofore unknown spectrum happens to be in need of measurement.)

To provide a synopsis of the information typically forwarded by the detector in the acquisition mode, we have to call again on the graphic capabilities of the manipulation software. Fig. 7 shows a "3-D" representation, with axis labels added manually and with each peak defined according to its FPD-active element. The chromatographic traces are smoothed by digital filtering and sent to the printer, not as a window dump but in (graphically) high resolution.

3.5. Use of chromspec readouts

The likes of Fig. 7 can serve as overviews of particular separations. Such graphs allow the operator to decide at a glance what spectral region(s) best to use for single-wavelength analysis and report. This task can be carried out directly, *i.e.* with the stored segment serving as the data base; or, requiring a second run, with the wheel stopped at the desired wavelength; or, if sensitivity is the overriding issue but additional work is not, with a suitable fixed-wavelength interference filter mounted in a conventional FPD channel. Further information might be obtained from such 3-D representations about the spectral behaviour of the solvent peak and the baseline and, more importantly, about the best spectral conditions at which to conduct quantitation, introduce matrix subtraction [9], improve selectivity vis-a-vis other sample components, and produce response-ratio [10] or CONDAC [11] chromatograms.

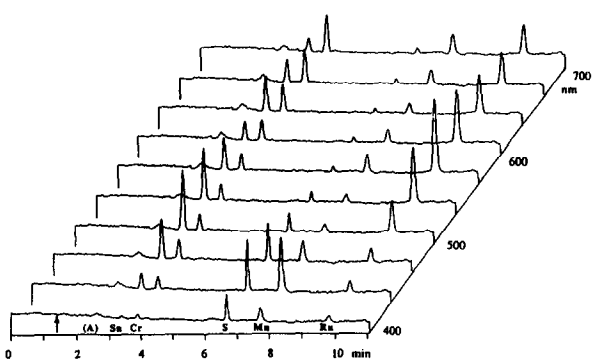

Fig. 7. A typical "3-D" separation. Compounds: A = 1 μl acetone (solvent); Sn = tetramethyltin; Cr = chromiumhexacarbonyl; S = di-*tert.*-butyldisulphide; Mn = methylcyclopentadienylmanganesetricarbonyl; Ru = ruthenocene. Hydrogen 30 ml/min, air 80 ml/min. First segment intensity multiplied by two. Graphic high-resolution mode. Labels added.

CONDAC ("conditional access") chromatograms use the distinct response ratios characteristic of FPD-active elements to accept peaks of only one element and reject all others. An example, which uses the data of Fig. 7, is shown in Fig. 8. The analyst is offered wide reign by the current ten (as compared to the earlier two [9–11]) channels: several spectrally different conditions are now available for producing background-corrected, element-specific or otherwise correlated chromatograms.

It is even easy to leaf through the spectral envelopes (which are stacked parallel to the *y* axis in Fig. 7) for tentative identification of

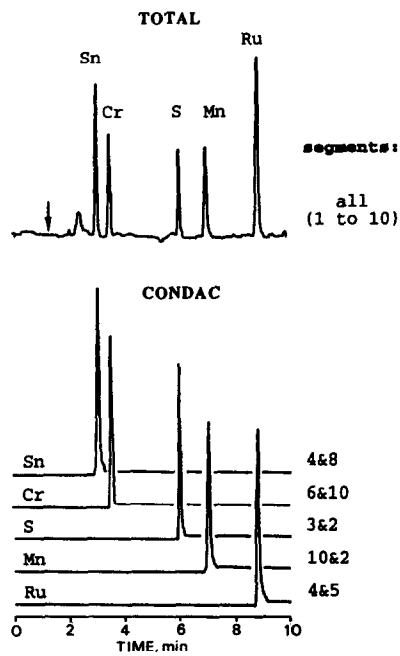

Fig. 8. Typical CONDAC [11] chromatograms from various segment combinations as indicated. Compounds: Sn = 2 ng tetramethyltin; Cr = 10 ng chromiumhexacarbonyl; S = 6 ng di-*tert.*-butyldisulphide; Mn = 20 ng methylcyclopentadienylmanganesetricarbonyl; Ru = 5 ng ruthenocene. Hydrogen 300 ml/min, air 80 ml/min. Without quartz chimney.

elements, for detailed comparison of spectrally similar peaks or for temporal assessment of peak purity. It may be justifiedly asked in this context why we did not portray the chromspec data in the customary protuberant 3-D topography. While easy to obtain, such technicoloured portraits may have turned out more confusing than revealing. Being staid chromatographers, we decided to outline only the chromatograms (time dimension) and leave the spectra (colour dimension) to the imagination of the viewer. Still, even a simple 3-D chromspec plot such as Fig. 7 efficiently represents the essence of the chromatographic and spectral information that is being collected by the acquisition program. Clearly the 3-D plot comprises more and broader information than the conventional, *i.e.* 2-D, chromatogram or spectrum.

3.6. 3-D vs. 2-D: the spectral dimension

Although analysts (or instrument companies) generally prefer 3-D to 2-D —that is, more information (or potential profit) to less— it must be noted that a higher number of physical or chemical dimensions can also mean a shorter or noisier range for any or all of them. In other words, a compromise has to be reached among the various instrumental settings that influence analytical and spectral performance.

Just to mention one example: the number of spectral segments (simultaneous chromatograms) is linked to the spectral resolution on one hand, and the useable signal range on the other. Obviously, the greater the number of segments the higher the spectral resolution. In a semicircular variable filter, divided into ten equitemporal segments during one revolution of the wheel mount, each segment can be monitored at most 5% of the time. Unless $1/f$ noise prevails —which it does not in our case— this means a loss in S/N ratio as compared to a conventional FPD channel. This loss will generally increase with the total number of segments available. In turn, the lower the S/N ratio the less precise the analysis and the shorter its working range. The addition of spectral information thus brings with it a deletion of the lowest part of the calibration curve, *i.e.* a shortening of the response dimension.

Further insight into the analytical quality of data from the acquisition mode can be obtained by using the manipulation mode's "TRICHROM" routine. In this routine the screen displays three chromatograms selected by the operator. To facilitate orientation, a "total" chromatogram, *i.e.* the sum of all ten segment chromatograms (divided by 10 to fit the screen) is usually selected as one of the three. The operator can scale (compress or expand) either the intensity axis or the time axis or both. In the former case, the signal "magnification factor" appears on the left side of the chromatogram. Fig. 9 shows a typical example of a "total" plus two segment chromatograms in the form of a window-dump. Note that the window-dump, while including some function buttons, does not include the constantly updated information that appears automatically on the bottom of the screen to keep the operator informed of the true chromatographic retention time and signal intensity.

To have available ten chromatograms from different wavelengths (or any time slice or additive/subtractive combination thereof, as obtained conveniently by using the "PIZZA" routine of the manipulation program) allows the operator to select the segments that offer the best selectivity, matrix suppression, quantitation, etc. If different peaks contain different heteroelements, the latter can be identified and processed at suitably different wavelengths. If a peak contains more than one FPD-active heteroelement, the elemental ratio can be estimated (similar to the classic case of thiophosphates [12]).

Several other, less obvious advantages may be hidden in this gratuitously available spectral information. For instance, the 3-D FPD may allow the operator to understand and perhaps even control the chemical nature of the baseline (background luminescence). Certain luminescent features may be intrinsic (*e.g.* arise from the oxyhydrogen flame), but many others may be extrinsic (*e.g.* derive from stationary phase bleed during temperature programming; from carrier

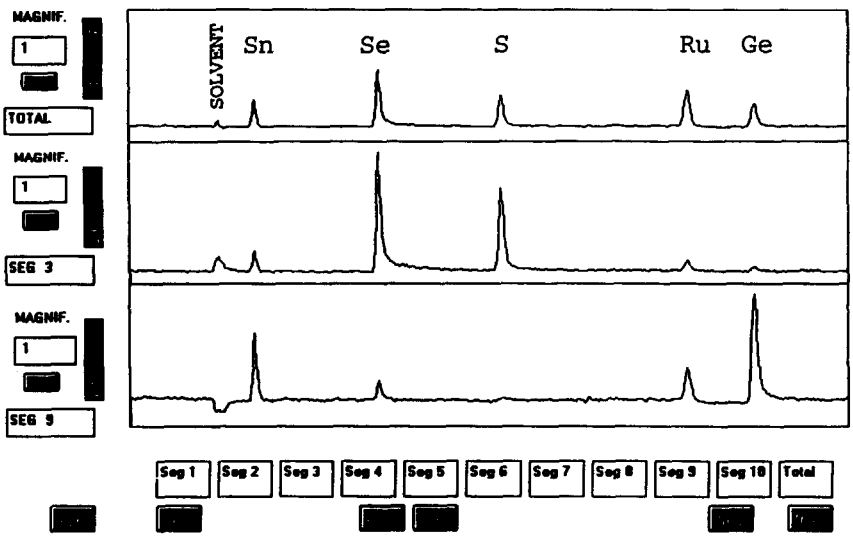

Fig. 9. A typical "TRICHROM" display used for data comparison and manipulation (window-dump only), from the chromatographic run shown in Fig. 5.

gas contamination; or, most insidiously, from injection port, column or detector memory). Our preliminary experience with the wheel system strongly suggests the presence of such temporary effects (which are, of course, also present in the 2-D FPD, but go unnoticed there). For instance, the spectral envelope of the baseline luminescence often changes from evening to morning and, less surprisingly, from one experimental series to the other. Also, the 3-D FPD may allow the operator insight into the behaviour of certain species that at the same time luminesce and quench luminescence —their own and that of other analytes— as in the well-known case of hydrocarbonaceous matrices [3,4,13].

There is little doubt that the immediate state of the FPD influences analyte response in various ways. Willy-nilly, once the computer starts turning out background spectra alongside analyte spectra, the former will be noticed and, in turn, benefit the latter —not just for the obvious spectral correction routines, but also for the diagnostic and prophylactic value of treating contaminating samples and contaminated detectors. However, only time will tell whether such information on potential background interferences and undesirable detector memories will prove a panacea for analysis or merely a placebo for the analyst.

3.7. 3-D vs. 2-D: the S/N ratio

The primary reason for Fig. 9 to be shown here is the visual appearance of the chromatograms, the selectivity they represent, the range of information they convey and —as a hint only— the breadth of manipulation they invite. However, opening a new dimension would be meaningless without ensuring that its sensitivity is up to its tasks. Under typical FPD conditions, the sensitivity of the wheel will almost unavoidably be lower than that of a conventional channel —but the important question is by how much. (If baseline noise were exclusively due to flame flicker, or to other slow chemical and chromatographic fluctuations, detection limits for the regular and the 3-D channel would obviously be comparable.)

When the filter wheel is simply inserted between the original Shimadzu cooling connector and the PMT housing, large amounts of various compounds have to be injected to be seen. This is due to a variety of reasons; some major, some minor. To start with a minor one: the new signal

path (from high-speed amplifier to ADC to digital filter to printer) produces S/N ratios that are estimated to be worse (by a factor of about two) than those from the old signal path (from electrometer to analog filter to stripchart recorder —both starting from the same flame and wheel arrangement, of course).

That a rotating filter produces lower S/N ratios than a stationary one is fairly obvious under shot-noise-limited conditions. What may be less obvious, however, is that the extent of this effect depends on the spectral nature of the measured peak. The largest difference between the filter rotating and the filter stationary occurs when the peak emits in only one of the ten wavelength regions; if, on the other hand, its emission is spread out over all ten, the difference is smaller. A similar argument obtains in the comparison of the "best segment" *vs.* the "total" chromatogram from the rotating filter. If the peak consists of a spectral continuum, the S/N ratio of the single wavelength segment is decidedly lower than that of all ten segments combined; if the peak consists of a sharp spectral feature, the opposite may be the case.

If we are willing to assume an idealized set of circumstances, *e.g.* that the noise is random, that electronic and timing effects are negligible, and so forth and so on, it becomes easy to put numbers to these various relationships [14]. A factor of three ($10^{1/2}$) is most often present in such theoretical comparisons. In actual cases it should be less; and in no case should it exceed ten. Exploratory experiments carried out with the filter rotating *vs.* stationary, and with compounds of manganese *vs.* ruthenium, are generally in agreement with these theoretical estimates. Observed from a different experimental angle, the "total" chromatogram from the rotating filter wheel (via the computer) has an S/N ratio that is, generally and typically, three to four times worse than that of the stationary filter wheel (via the electrometer).

3.8. A detour: FPD noise characteristics

We should include at this point a consideration that, though largely speculative, is of particular importance for the wheel system. Earlier we had mentioned that the S/N ratio cannot be improved in the case of flame flicker. That is conventional wisdom for a single-channel instrument such as the common FPD, but is not necessarily true for dual- or multiple-wavelength instruments. If noise, regardless of its origin, should contain components of a frequency lower than the temporal resolution of the monitoring system, such components could be effectively suppressed to produce a higher S/N ratio.

Typical chromatograms like those shown in Figs. 5, 7 and 9 are electronically filtered to remove fast noise; however, sizeable amounts of apparently slow noise are still in evidence. Noise components with frequencies near that of the analyte peak can obviously not be removed by simple data smoothing. They could, however, be removed by the subtraction capability of the PIZZA menu (as well as by a variety of other techniques). Our peaks are generally wider than 10 s, while our temporal resolution of the raw data, in the worse case, is narrower than 100 ms: this seems to offer an opportunity to improve the S/N ratio. (It also offered the bait that lured us into attempting correlated dual-channel chromatography some years ago: our earlier two-PMT attempt to reduce noise failed —but the experimental set-up, once in existence, earned its keep by offering other analytically meritorious features [9,15]).

In the case of the spectral wheel, the present one-PMT attempt to reduce noise by subtracting scaled segment chromatograms failed likewise. In fact, the noise of the subtraction chromatogram was larger than the noise of either of the two constituent chromatograms; by a factor close to the square root of two. That number suggests random, uncorrelated noise. But how can noise with a time constant above, say, 1 s not be correlated, *i.e.* not be simultaneously present in two channels whose segment acquisition time is only 5 ms and whose repetition time is only 100 ms?

A plausible answer is that the "true" (= initial) noise contains, in fact, no low-frequency components —at least none strong enough to make a difference. What appears as

low-frequency components in Figs. 5, 7 and 9 (as well as in the later Fig. 10) is really the result of random fluctuations that are fast enough (>200 Hz) to escape correlation by the wheel. These uncorrelated fast fluctuations (after summation by the gated integrator) merge during the data-smoothing process into the much slower fluctuations *unique* to each segment. This later type of noise, in contrast to genuine flame flicker, PMT drift, etc., cannot be cancelled by time/wavelength multiplexing. While operational distinctions between initial and filtered noise are rarely drawn, and consequences of noise frequency shifts on baseline correction and detection limits rarely explored, they are of obvious importance for the present case. For one, they can help the analyst decide which S/N losses can be avoided or ameliorated, and which can not.

3.9. 3-D vs. 2-D: detection limits

The major S/N loss is due to the diminution of light on its way from the flame to the PMT tube. When the wheel is merely being inserted between the existing detector block (including the connecting light tunnel carrying the cooling coils) and the existing PMT housing, the S/N ratio is very poor. With *all* the mechanical and optical adjustments described in the Experimental section in place, the S/N ratio improves about fifty-fold (as measured with ruthenocene).

Yet, the improved FPD channel with wheel is still not quite as sensitive as the conventional FPD channel without, an experimental finding easily anticipated on optic and electronic grounds. While as authors we could be considered obliged to put hard numbers to this difference in sensitivity, it should be understood that any such number may depend heavily on the nature of the element being tested and the flow conditions chosen to test it. The most meaningful comparison indeed should be one that is typical in its scope, reasonable in its execution and fair in its assessment.

One such proof-of-the-pudding comparison can be carried out by simply determining the detection limits of a few sensitive and, in their spectral behaviour, disparate elements with the rotating filter wheel; and to use just a *single* segment (which corresponds to monitoring the flame at a given wavelength only 5% of the time) for the calculation. The conditions for this test of detector performance are those suited to each *individual* element: the results can hence be legitimately compared with the known detection limits of the same elements as determined at optimized conditions in the conventional FPD. The two old FPD protagonists, phosphorus and sulphur, appear in their familiar roles. The deuteragonists germanium and ruthenium are less familiar actors on the analytical stage, but are included here to round out the cast. In a series of four separate runs, 100 pg of tris(pentafluorophenyl)phosphine, 1 ng of thianaphthene (benzo[*b*]thiophene), 500 pg of tetra-*n*-butylgermanium and 100 pg of ruthenocene are tested in individually optimized settings.

In the case of sulphur, a narrow quartz chimney surrounds the detector jet, and the flow conditions are those that suit the S_2 emission (the conventional quadratic sulphur response of the FPD [1–4, *cf.* ref. 16]). The quartz chimney is also used for phosphorus and germanium, but is removed for ruthenium. Phosphorus is tested last to minimize possible detector contamination.

The $S/RMS = 3$ detection limits for one-segment chromatograms in the rotating-wheel FPD arrangement are $1 \cdot 10^{-11}$ g tris(pentafluorophenyl)phosphine or $2 \cdot 10^{-13}$ g P/s for phosphorus (via HPO*), $8 \cdot 10^{-11}$ g thianaphthene or $9 \cdot 10^{-12}$ g S/s for sulphur (S_2^*), $3 \cdot 10^{-11}$ g tetra-*n*-butylgermanium or $2 \cdot 10^{-12}$ g Ge/s for germanium (GeH*) and $2 \cdot 10^{-11}$ g ruthenocene or $2 \cdot 10^{-12}$ g Ru/s for ruthenium. The $S/N_{p\text{-}p} = 2$ detection limits are $7 \cdot 10^{-13}$ g P/s, $3 \cdot 10^{-11}$ g S/s, $7 \cdot 10^{-12}$ g Ge/s and $4 \cdot 10^{-12}$ g Ru/s. (The numbers for sulphur may be low since the computer-based calculation of the detection limit uses a *linear* extrapolation. However, many calibration curves for "quadratic" sulphur actually do become linear as they approach the minimum detectable amount.)

For general comparison: Dressler [3] states that "the minimum detectable mass rate ranges from about $1 \cdot 10^{-13}$ g/s to $2 \cdot 10^{-12}$ g/s of P for phosphorus compounds and from about $2 \cdot 10^{-12}$

g/s to $5 \cdot 10^{-11}$ g/s of S for sulphur compounds" (his reference numbers deleted). Our own group —using the same but then much younger gas chromatograph— found the relevant minimum detectable flows at $S/N_{p\text{-}p} = 2$ to be $2 \cdot 10^{-13}$ g Ge/s (as GeH) [17], and $4 \cdot 10^{-13}$ g Ru/s (at 526 nm; emitter unidentified but possibly RuH) [18].

The corresponding detection limits from the wheel are by no means the lowest possible, but are those we consider reasonable under the circumstances. What is "possible" in this context and what "reasonable" needs to be briefly discussed in order to allow the reader an informed evaluation of the quoted figures of merit.

Since most emissions in the FPD cover several segments (compare Fig. 6), the one-segment limits of detection are generally worse than those of multi-segment or all-segment, (*i.e.* "total") chromatograms. This is analogous to the behaviour of the conventional FPD operating with a narrowband *vs.* a broadband *vs.* no interference filter. The rotating wheel is therefore being evaluated in this regard on a *worst*-performance basis. Yet the *single*-segment detection limit is closer in spectral nature to that of the conventional, *i.e.* fixed-wavelength FPD. Also, there may be good practical reasons for using a *single*-segment chromatogram despite its poorer sensitivity: its *selectivity* is more often than not higher than that of the "total" chromatogram.

The detailed calculation of detection limits has been described in the Experimental section. Note that the wider term "detection limit" denotes a computer routine that, in our case, characterizes *detector* performance; this differs from the narrower literature definition which refers to a *total* analytical method [19]. In order to remain "reasonable", data smoothing is restricted here to settings that reduce the analyte peak height by no more than 10% —despite the fact that higher S/N ratios can be obtained if that restriction is ignored. The baseline interval used for the measurement of noise spans about twenty standard deviations of the analyte peak.

Comparisons between detection limits of segmented (3-D FPD) *vs.* continuous (2-D FPD) response reveal some interesting differences. For instance, the conversion factors between the *RMS*- and $N_{p\text{-}p}$-based types of detection limits differ, suggesting a different character (distribution) of noise for 3-D and 2-D modes. Also, the conversion factor between the two definitions clearly depends on the extent of data smoothing. The detailed description/explanation of such effects is, however, lengthy and not essential to this paper; it will be given elsewhere [20].

While in our role as authors we have become habituated to reporting *two* types of detection limits, each for both injected mass and detected flow of analyte, we have been doing so primarily to placate the discriminating referee and accommodate the inquiring reviewer. Left to our own predilections, however, we would simply provide a typical chromatographic peak with enough noise around, *i.e.* a chromatogram taken within range of the detection limit. For any kindred chromatographer bent on carrying out detectability and noise assessments according to personal or local preferences, we therefore offer in Fig. 10 some single-segment peaks from the rotating filter wheel. Segment numbers and 1-min time units are indicated on the individual abscissae. These chromatograms are FIR-filtered; however, AVG and RC filters would have produced very similar results [20].

From this comparison it seems that (very approximately and highly analyte- and condition-dependent) the new 3-D FPD is about one decade less sensitive than the conventional 2-D FPD and that, consequently, its linear range is about one power-of-ten shorter. That loss seems reasonable at the present state of affairs, given that the absolute light level of chemiluminescence is low and that "noise", primarily if not exclusively, appears to consist of photon shot noise [14].

In comparison with a regular 2-D FPD channel, the 3-D FPD's high-speed electronics may contribute to S/N loss by a factor around 2 (a mainly experimental estimate); and the 5% dwell time for each segment could be considered responsible for a loss factor of $(100/5)^{1/2} = 4.5$ (given a square-root dependence of the S/N ratio on sampling time). The light transmission of the variable filter is lower than that of a typical fixed-wavelength interference filter, and the need

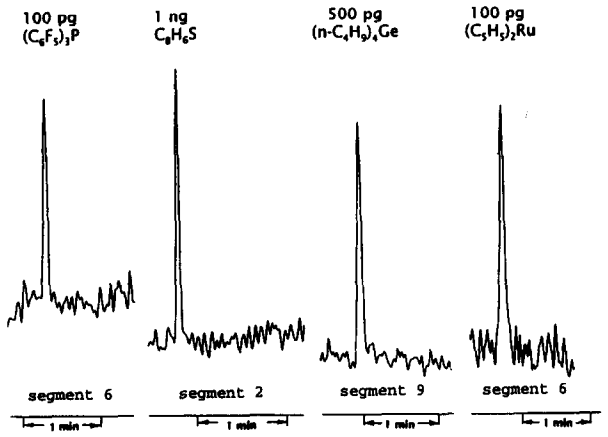

Fig. 10. Typical single-segment peaks near the detection limit. Composite picture in graphically high-resolution mode from selected windows at different wavelength regions (segment numbers), flow conditions, extents of background luminescence, and time scales. Tetraethyllead injections were used prior to the experiment to reduce the luminescent background. Compounds and conditions from left to right (all flows in ml/min): 100 pg tris(pentafluorophenyl)phosphine, 200 hydrogen, 40 air, PMT −860 V, quartz chimney present, variable filter segment 6; 1 ng thianaphthene, 50 hydrogen, 30 air, PMT −830 V, chimney present, segment 2; 500 pg tetra-*n*-butylgermanium, 50 hydrogen, 40 air, PMT −830 V, chimney present, segment 9; 100 pg ruthenocene, 300 hydrogen, 80 air, PMT −800 V, chimney absent, segment 6. Data are FIR filtered close to a 10% reduction in analyte peak height.

to focus the poorly defined beam on the variable filter through not too wide an aperture must add to the photon deficit. On the other side of the ledger, centering the flame and backing it up by a mirror improves light throughput considerably (this may also help a conventional FPD channel although, because of the shorter light path and the much higher light level of the latter, far less so than the wheel system). While matters of sensitivity are condition- and analyte-dependent, and by far not as straightforward as they are made to appear in this short account, the nigh inevitable one-order-of-magnitude loss seems a relatively minor (and still introductory) price to pay for the value added.

But this also invites a value-added tax to be imposed on the goods and services the FPD offers: when the rotating variable interference filter adds wavelength as an instantaneous third dimension to the FPD, it also increases its complexity and hence its acquisition and maintenance costs. In our case, the main initial cost was the US$ 1000 filter itself. A suitable computer/monitor/printer combination may be available second-hand in many laboratories; newly purchased it would require an additional US$ 2000. This seems commensurate with the price of a simple gas chromatograph with single-channel FPD (about US$ 10 000).

Whether a lower sensitivity, a higher price, and a greater complexity can be justified by the information content of a third, spectral dimension has yet to be determined (and should in any case be heavily dependent on the particular analytical demands and conditions). It would appear, however, that the revolving spectral wheel may yet provide one of the simplest and least expensive third dimensions ever added to analytical instrumentation.

3.10. A different type of filter wheel?

The wheel is, however, still far from perfect. Light throughput, hence sensitivity, could undoubtedly be improved. Also, the available wavelength range could be changed to serve particular analytical requirements, for instance by installing custom-made variable filters of smaller, wider, or simply different (*e.g.* UV, IR) optical range. Yet, a *variable-wavelength* filter may, in fact, not be the best choice for many analytical applications.

A possibly better arrangement may involve conventional *fixed-wavelength* 1-in. diameter interference filters held in, say, eight filter holders set in close proximity and radial symmetry over 360° into a metal wheel, with eight acquisition triggers commensurately positioned on (or, alternatively, with eight holes drilled through) its rim to intercept (or pass) the IR trigger beam. In this manner, a variety of advantages could be realized. First, no acquisition time would be "wasted" on an opaque semicircle, or on wavelength regions of only minor interest (as is the case now). Second, any wavelength (*e.g.* typically optimized FPD wavelengths such as 394 or 405 nm for S_2^*, 525 nm for HPO*, etc.) could be

used —and these could range from UV to IR. Third, such conventional filters would inherently produce better resolution (*i.e.* their bandpass, typically 10 nm, would not be degraded by temporal segmentation or beam spread effects). Also, their transmission would typically be better than that of the variable filter. Fourth, the choice which wavelengths to monitor could be adjusted perfectly (subject only to the availability of filters) to analytical tasks (such as background correction and other correlational approaches [9–11]) that rely on the constancy of spectral response ratios [21]. Fifth, a wheel of this nature could also be used for many non-chromatographic purposes, *e.g.* analyzing simple solutions [Na, K, Ca, etc. (*cf.* ref. 22)] by flame photometry, monitoring spectrally classifiable meteorological and astronomical events, following and/or stimulating the response of bioluminescent communities, testing various types of weak natural or stimulated luminescences in inorganic materials, etc. Sixth, the wheel could serve equally well as a (computer-controlled, multiwavelength, pulsed) light *source*. Several other applications seem fairly obvious.

Though sorely tempted to do so, our group shall not be able to develop further wheels, owing to current constraints on electronic and programming support. We do hope, however, that other laboratories see fit to put their own spin on this interesting topic.

Acknowledgements

This research was financially supported by NSERC grant A-9604. The suggestions and highly skilled support by the Department's Machine Shop (Cecil Eisener) and Electronics Shop (Chris Wright) are gratefully acknowledged. Without their help, this study would not have been possible. Thanks are also due to H. Singh for help in revising this manuscript.

References

[1] S.S. Brody and J.E. Chaney, *J. Gas Chromatogr.*, 4 (1966) 42.
[2] S. Kapila, D.O. Duebelbeis, S.E. Manahan, in R.M. Harrison and S. Rapsomanikis (Editors), *Environmental Analysis Using Chromatography Interfaced with Atomic Spectroscopy (Ellis Horwood Series in Analytical Chemistry)*, Wiley, Chichester, 1989, pp. 76–95.
[3] M. Dressler, *Selective Gas Chromatographic Detectors (Journal of Chromatography Library*, Vol. 36) Elsevier, Amsterdam, 1986, pp. 133–160.
[4] S.O. Farwell and C.J. Barinaga, *J. Chromatogr. Sci.*, 24 (1986) 483.
[5] P.W. Grant, in D.H. Desty (Editor), *Gas Chromatography 1958 (Proc. Symp., Amsterdam, May 1958)*, Butterworth, London, 1958, pp. 153–163; as cited in D. Jentzsch and E. Otte, *Detektoren in der Gas-Chromatographie*, Akademische Verlagsgesellschaft, Frankfurt/Main, 1970, pp. 177–178.
[6] P.L. Patterson, R.L. Howe and A. Abu-Shumays, *Anal. Chem.*, 50 (1978) 339.
[7] M.L. Selucky, *Chromatographia*, 4 (1971) 425.
[8] K.W. Busch and M.A. Busch, *Multielement Detection Systems for Spectrochemical Analysis*, Wiley, New York, 1990, pp. 612–613.
[9] W.A. Aue, B. Millier and X.-Y. Sun, *Can. J. Chem.*, 70 (1992) 1143.
[10] B. Millier, X.-Y. Sun and W.A. Aue, *Anal. Chem.*, 65 (1993) 104.
[11] W.A. Aue, B. Millier and X.-Y. Sun, *Anal. Chem.*, 63 (1991) 2951.
[12] M.C. Bowman and M. Beroza, *Anal. Chem.*, 40 (1968) 1448.
[13] W.A. Aue and X.-Y. Sun, *J. Chromatogr.*, 641 (1993) 291.
[14] J.D. Ingle, Jr. and S.R. Crouch, *Spectrochemical Analysis*, Prentice Hall, Englewood Cliffs, NJ, 1988, Ch. 5.
[15] W.A. Aue, B. Millier and X.-Y. Sun, *Anal. Chem.*, 62 (1990) 2453.
[16] W.A. Aue and X.-Y. Sun, *J. Chromatogr.*, 633 (1993) 151.
[17] C.G. Flinn and W.A. Aue, *J. Chromatogr.*, 186 (1979) 299.
[18] X.-Y. Sun and W.A. Aue, *Can. J. Chem.*, 67 (1989) 897.
[19] Analytical Methods Committee, Royal Society of Chemistry, *Analyst*, 112 (1987) 199.
[20] X.-Y. Sun, B. Millier, C.W. Warren, H. Singh and W.A. Aue, *J. Chromatogr.*, submitted for publication.
[21] X.-Y. Sun and W.A. Aue, *J. Chromatogr. A*, 667 (1994) 191.
[22] F.W.J. Garton, J.L. Waddingham, P.C. Wildy, H.M. Davis and S.I. Hawkins, *U.K.A.E.A. Res. Rep. AERE R4141*; as cited in J.B. Dawson, D.J. Ellis and R. Milner, *Spectrochim. Acta*, 23B (1968) 695.